

# Study of SOFC Operational Behavior by Applying In-Situ Diagnostic Methods

Günter Schiller, Wolfgang Bessler, Caroline Willich, K. Andreas Friedrich  
Deutsches Zentrum für Luft- und Raumfahrt (DLR)  
Institut für Technische Thermodynamik  
Pfaffenwaldring 38-40, D-70569 Stuttgart, Germany  
Tel.: +49-711-6862635  
Fax: +49-711-6862747  
guenter.schiller@dlr.de

## INTRODUCTION

High electrical performance and long lifetime are key requirements that must be fulfilled for a successful introduction of fuel cells into the market. For achieving a high efficiency, a high fuel utilization is required. This requirement, on the other hand, results in strong concentration gradients at the anode where the fuel is successively diluted by reaction products during the reaction process and, hence, in an inhomogeneous distribution of electrochemical performance and temperature. Inhomogeneous distributions of electrochemical and thermal properties such as local power density and local temperature might detrimentally affect both efficiency and long-term durability through thermo-mechanical stress and degradation phenomena. In order to optimize the operational behavior of fuel cells and minimize cell degradation the application of advanced diagnostic methods by monitoring cell characteristics under real operating conditions can provide detailed information about the spatial distribution of the electrical, chemical and thermal cell properties. DLR has developed spatially resolved diagnostic techniques with a segmented cell arrangement where different techniques such as IV characteristics, impedance spectroscopy, gas chromatography and temperature measurement are involved [1, 2]. The segmented cell setup allows a largely extended insight into fuel cell processes both for increasing the fundamental understanding and for optimizing cell and flow field design. The obtained data can be used for mathematical modeling and model validation and for predicting physical, electrochemical and fluid mechanical properties [3, 4]. Recently, imaging techniques such as optical microscopy and Raman spectroscopy have been additionally adopted for in-situ observation of fuel cells. The paper gives an overview of in-situ diagnostic methods applied at DLR Stuttgart for the determination of local effects and the identification of critical operating conditions during technically relevant SOFC operation. Exemplary results from experimental investigations are presented.

## EXPERIMENTAL

The measurement setup for segmented cells as developed at DLR Stuttgart is shown schematically in Fig. 1. It allows for the integral and spatially resolved measurement of current density and voltage, the local and integral determination of impedance data, the local measurement of temperature and temperature distribution and the spatially resolved analysis of the fuel gas concentrations along the flow path. Square-shaped as well as rectangular cells with an area of  $100 \text{ cm}^2$  are divided into 16 segments with an active area of each segment of  $4.84 \text{ cm}^2$  and  $3.78 \text{ cm}^2$ , respectively. The cells are integrated in a metallic cell housing and sealed with glass seal. The metallic housing is also subdivided into 16 galvanically isolated segments. In order to determine the temperature at each segment, thermocouples are introduced in the metallic segments. Additionally, capillary tubes that correspond to the cathodic segments are integrated at the anode side at 16 measuring points to take samples of the anode gas to be analyzed by gas chromatography. The setup is flexible with regard to the integration of different cell designs. Metal-supported cells (MSC), as they are developed and fabricated in house according to the DLR spray concept [5], as well as electrolyte-supported cells (ESC) and anode-supported cells (ASC) can be characterized. With MSC and ASC, only the cathode is segmented, whereas ESCs are segmented on both the anode and the cathode side. For the contact of the electrodes Ni and Pt meshes were used. More details on the measurement system are given in [2].

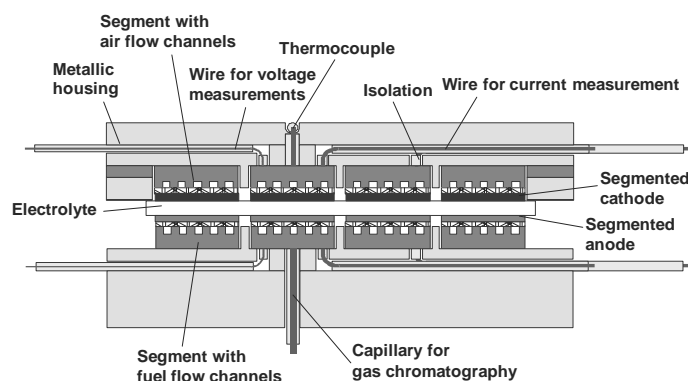


Fig. 1: Setup of measurement system for the characterization of segmented cells

## RESULTS AND DISCUSSION

The measuring system described has been applied to locally characterize SOFCs with the segmented cell arrangement. Two examples are given to demonstrate the potential of this spatially resolved measuring technique.

### Investigation of an anode-supported cell (ASC) with high fuel utilization

A segmented anode-supported cell (ASC) containing a 540  $\mu\text{m}$  thick NiO/YSZ anode with a thin anode functional layer, a 7  $\mu\text{m}$  thick 8YSZ electrolyte, a 7  $\mu\text{m}$  thick YDC interlayer and a 30  $\mu\text{m}$  thick LSCF cathode was operated under a condition with high fuel utilization. The anode was fed with 33 %  $\text{H}_2$ , 1 %  $\text{H}_2\text{O}$  and 66 %  $\text{N}_2$ . This condition was chosen in order to simulate nitrogen-rich reformat gas. The cathode was fed with air in counter-flow operation.

The measured two-dimensional distribution of power density at 800  $^\circ\text{C}$  in the 16 segments is shown in Fig. 2 for an average power density of 460  $\text{mW}/\text{cm}^2$ . The fuel utilization at this condition is 80 %. The cell performance is strongly inhomogeneous, with the power density systematically decreasing from fuel inlet (left side of Fig. 2) to fuel outlet (right side of Fig.2). It will be shown below that this decrease is due to fuel depletion along the flow path. Moreover, there is a notable difference for the four segment rows (upper row to lower row in Figure 2). This difference may be due to sealing issues or inhomogeneous gas supply to the gas channels. Further segment-to-segment scattering is likely due to a variation in contact resistance which may also lead to systematic row-to-row variations when the contact pressure is inhomogeneous. For comparison with the model (which represents the behavior along one single channel), the row with segments 9-12 was chosen.

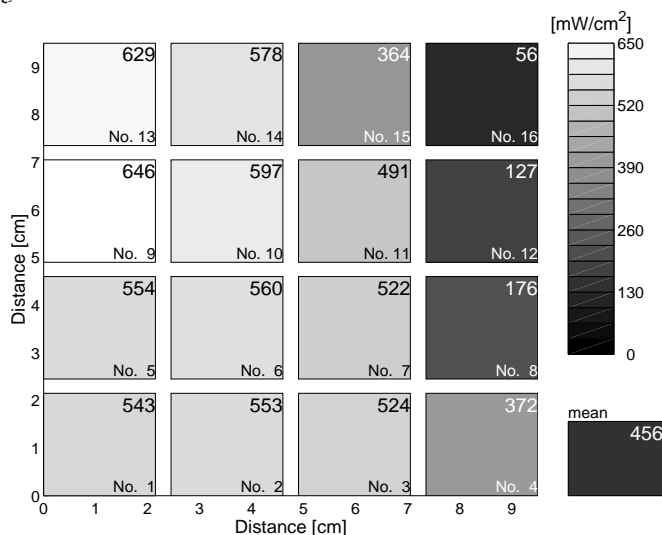


Fig. 2: Measured two-dimensional distribution of power density over the 16 segments under operating conditions with high fuel utilization (counter-flow operation; anode: 33 %  $\text{H}_2$ , 1 %  $\text{H}_2\text{O}$ , 66 %  $\text{N}_2$  in  $\text{H}_2$ , 1.1 m/s inflow velocity; cathode: air, 5.2 m/s inflow velocity;  $T = 800$   $^\circ\text{C}$ ) at an average cell voltage of 0.59 V. The fuel inlet is on the left side, the air inlet at the right side.

Experimental and simulated global and local current-voltage characteristics for segments 9-12 are shown in Fig. 3. Simulations were performed using a 2D model along one representative channel and through the thickness of the MEA. This detailed 1D+1D elementary kinetic electrochemical model represents one single channel of the experimental setup. One-dimensional channel flow ( $x$  dimension) is described using the Navier-Stokes conservation equations (continuity, species, momentum), corresponding essentially to a plug-flow model with axial diffusion. One-dimensional mass transport through the membrane-electrode assembly (MEA) ( $y$  dimension) is described by coupled Fickian/Knudsen diffusion and Darcy flow. Charge transport in the solid electrolyte and the electrolyte phase of the composite electrodes is described in two dimensions using Ohm's law. Details about the used model are described in [3].

The global IV-curve (Fig. 3a) shows a typical shape with a parabolic behavior at low currents, linear behavior at intermediate currents, and a limiting current density of  $\sim 0.8$   $\text{A}/\text{cm}^2$  at high currents. The maximum power density ( $P_{\text{max}} = 470$   $\text{mW}/\text{cm}^2$ ) is observed at a global cell voltage of 0.70 V. Local IV-curves for segments 9-12 are represented by plotting local segment voltage versus local segment current (Fig. 3b). The local behavior shows a considerable variation of current density for different cell segments. At high polarization, segments 11 and 12 that are located close to the fuel outlet show a particularly interesting behavior: the current decreases while at the same time the segment voltage strongly decreases. This "inverse" behavior is due to strong fuel depletion. At the same time, the current density of segment 9 that is located at the fuel inlet continues to increase. There is excellent quantitative agreement between model and experiment for both the local and the global behavior.

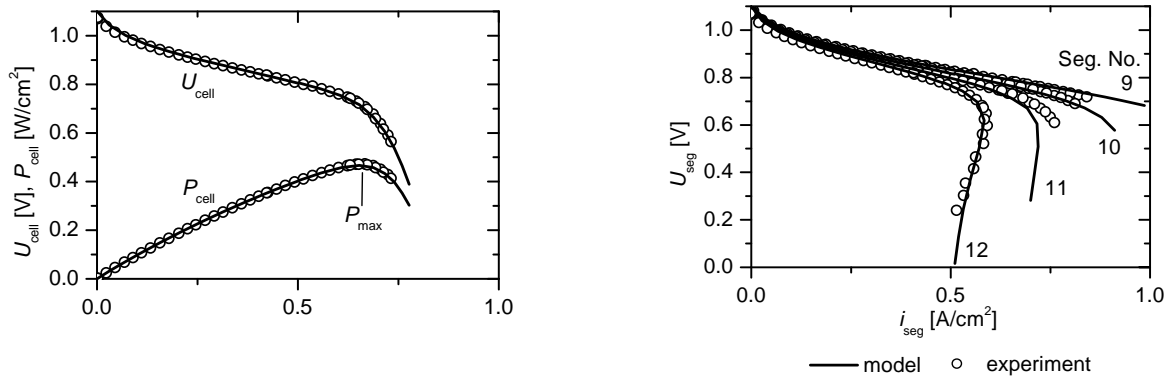


Fig. 3: Experimental and simulated polarization behavior for the segmented cell using the 2D model under operating conditions with high fuel utilization (counter-flow operation; anode: 33 % H<sub>2</sub>, 1 % H<sub>2</sub>O, 66 % N<sub>2</sub> in H<sub>2</sub>, 1.1 m/s inflow velocity; cathode: air, 5.2 m/s inflow velocity; T = 800 °C). (a) Global current-voltage curves, (b) local segment voltage versus local segment current. The numbers indicate the segments, where segment 9 is the first in flow direction of the fuel gas.

### Operation of an anode-supported cell (ASC) with reformat as fuel gas

This example covers the operation of an anode-supported cell with a reformat composition as the fuel gas and the electrochemical reaction of the fuel gas components along the flow path [7]. A spatially resolved measurement along the flow path of the fuel with a realistic reformat composition (54.9 % N<sub>2</sub>, 16.7 H<sub>2</sub>, 16.5 % CO, 6.6 % CH<sub>4</sub>, 2.2 % CO<sub>2</sub>, and 3.2 % H<sub>2</sub>O) was performed to investigate the processes taking place in more detail. The influence of the area-specific load on the power density and the fuel utilization at operation of a segmented ASC cell (counter-flow) along a row of segments (segment 9–12) with fuel inlet at segment 9 is shown in Fig. 4. The results in Fig. 4 reveal an excellent conversion of CO- and CH<sub>4</sub>-containing fuel gas with 78.1 % at 400 mA/cm<sup>2</sup> and with 83.9 % at 435 mA/cm<sup>2</sup> at the fuel exit. At a current density between 0 and 200 mA/cm<sup>2</sup> the power density decreases only slightly along the flow path, but at a load of 400 mA/cm<sup>2</sup> a quite significant and strong reduction of power density at the fuel exit (segment 12) was observed. This behavior is even more pronounced at a further increased current density of 435 mA/cm<sup>2</sup> of the total cell; segment 12 now shows a very low power density. It seems that the increasing conversion rate at the segments 9–11 causes performance reduction at segment 12 which could result in critical conditions and hence enhanced corrosion at the fuel exit.

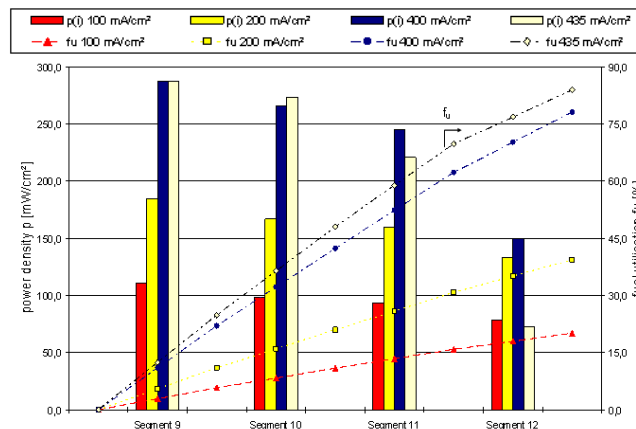


Fig. 4: Comparison of power density and fuel utilization along the flow path during variation of the area-specific load of an ASC cell (active area: 73.96 cm<sup>2</sup>) during operation with reformat gas; counter-flow mode, fuel gas inlet at segment 9, fuel gas outlet at segment 12; current density equivalent: 0.552 A/cm<sup>2</sup>, air flow rate: 0.02 slpm/cm<sup>2</sup>

In order to determine how the internal reforming of CH<sub>4</sub> which is a component of the reformat takes place, segments 9–12 were investigated at different current densities by means of gas chromatography measurements. These measurements showed clearly how the internal reforming of CH<sub>4</sub> increases with increasing current density. The increase of current density from 0 to 435 mA/cm<sup>2</sup> results in a higher conversion of H<sub>2</sub> to H<sub>2</sub>O and CO to CO<sub>2</sub>. A higher water content favors the shift and hence the reforming reaction. At 0 mA/cm<sup>2</sup> and 100 mA/cm<sup>2</sup> the water content drops at the segments 10 and 11 to almost 0%. The resulting diminished CO<sub>2</sub> and enhanced CO amount favors the Boudouard reaction and hence the carbon formation. With increasing current density above 100 mA/cm<sup>2</sup> the water content also increases continuously along the flow path thus avoiding critical conditions for the cell. At 200 mA/cm<sup>2</sup> methane is almost completely converted in the cell. With higher current density methane conversion is enhanced in direction of the fuel inlet. Due to the reforming of methane the hydrogen content at first increases at the fuel inlet at all current densities. At lower current densities and hence low conversion rates the hydrogen content is high whereas it decreases steadily at high current densities. The fuel utilizations calculated from the current densities correlate very well with the measured gas concentrations in the off-gas of the cell. More details on the investigation of internal reforming of CH<sub>4</sub> are reported in [7].

### Raman Spectroscopy and Optical Microscopy

The measurement setup for segmented cells described allows for the determination of gas concentrations by taking gas samples through tubes in the middle of each segment on the anode side and subsequent analysis by gas chromatography. A much higher

spatial resolution along the anode gas channel can be achieved by applying one-dimensional laser Raman spectroscopy. This optical technique can be applied for measuring in-situ the number densities of several molecular species simultaneously, thus enabling the determination of the composition and concentration of relevant gaseous species ( $H_2$ ,  $H_2O$ ,  $CH_4$ ,  $CO$ ,  $CO_2$ ,  $N_2$ ) within the flow channel of the anode with high spatial and temporal resolution. Solid-state Raman spectroscopy has been applied for studying SOFC processes ex-situ [8-9] but these studies were mainly devoted to the measurement of local temperature and mapping out of phase stability of solid electrode surfaces by monitoring the temporal variation of the oxidation state of materials. In our approach we apply in-situ gas-phase Raman spectroscopy of species concentrations and temperature during SOFC operation with technically relevant operating conditions.

In order to realize such measurements a new SOFC test rig has been built up which gives an optical access to the flow field of a SOFC cell setup through transparent windows in the furnace made of quartz glass as well as using a transparent anode flow field also entirely consisting of quartz glass. The laser system to be used for the Raman experiments at DLR consists of three double-pulse Nd:YAG lasers. The scattered light is collected at  $90^\circ$  with a grating spectrograph. The spectrally dispersed image of the beam is captured by a CCD camera. The objective of the experiments which have started in mid 2010 is the spatially resolved study of reactions taking place at the anode during SOFC operation under different operating conditions (variation of fuel gases including reformat compositions, temperature, fuel utilization) and the comparison with results obtained from electrochemical impedance spectroscopy. The setup also enables optical microscopy through the transparent optical access to the cell by means of a long-distance microscope and a CCD camera in order to image the electrode surface with high spatial and temporal resolution. It is intended to investigate in this way coke formation and carbon and sulphur poisoning. By applying these new techniques for in-situ observation of processes occurring during SOFC operation additional information and insight is expected for a better understanding of reactions and processes taking place under operational conditions.

## REFERENCES

1. P. Metzger, "Ortsaufgelöste Charakterisierung von Festelektrolyt-Brennstoffzellen (SOFC) durch Messung betriebsrelevanter Größen entlang des Strömungswegs", PhD Thesis, Universität Stuttgart, 2010
2. P. Metzger, K. A. Friedrich, H. Müller-Steinhagen, G. Schiller, "SOFC Characteristics along the Flow Path", *Solid State Ionics*, Vol. 177, pp. 2045-2051, 2006
3. W. G. Bessler, S. Gewies, C. Willich, G. Schiller, K. A. Friedrich, "Spatial Distribution of Electrochemical Performance in a Segmented SOFC: A Combined Modeling and Experimental Study", *Fuel Cells*, Vol. 10, No. 3, pp.411-418, 2010
4. G. Schiller, W. G. Bessler, K. A. Friedrich, S. Gewies, C. Willich, "Spatially Resolved Performance in a Segmented Planar SOFC", *ECS Transactions*, Vol. 17, No. 1, pp. 79-87, 2009
5. G. Schiller, R. Henne, M. Lang, M. Müller, "Development of Solid Oxide Fuel Cells by Applying DC and RF Plasma Deposition Technologies", *Fuel Cells*, Vol. 4, No. 1-2, pp. 56-61, 2004
6. P. Metzger, K. A. Friedrich, G. Schiller, H. Müller-Steinhagen, "Investigation of Locally Resolved SOFC Characteristics along the Flow Path", *ECS Transactions*, Vol. 7, No. 1, pp. 1841-1847, 2007
7. P. Metzger, K. A. Friedrich, G. Schiller, C. Willich, "Spatially Resolved Measuring Technique for SOFC", *Journal of Fuel Cell Science and Technology*, Vol. 6, No. 2, pp. 021304-1 - 021304-4, 2009
8. R. C. Maher, L. F. Cohen, P. Lohsoontorn, D. J. L. Brett, N. P. Brandon, "Raman Spectroscopy as a Probe for Temperature and Oxidation State for Gadolinium-Doped Ceria Used in Solid Oxide Fuel Cells", *J. Phys. Chem. A*, Vol. 112, pp. 1497-1501, 2008
9. M. P. Pomfret, J. C. Owrutsky, R. A. Walker, "High Temperature Raman Spectroscopy of Solid Oxide Fuel Cell Materials and Processes", *J. Phys. Chem. B*, Vol. 110, No. 35, pp. 17305-17308, 2006